GLOBAL-01209; No of Pages 18

Available online at www.sciencedirect.com

ScienceDirect

GLOBAL AND PLANETARY CHANGE

Global and Planetary Change xx (2006) xxx–xxx

www.elsevier.com/locate/gloplacha

Palaeoecological constraints on late Glacial and Holocene ice retreat in the Southern Andes (53°S)

Rolf Kilian [a,*], Christoph Schneider [b], Johannes Koch [c], Martinus Fesq-Martin [a], Harald Biester [d], Gino Casassa [e], Marcelo Arévalo [f], Gert Wendt [g], Oscar Baeza [a], Jan Behrmann [h]

[a] *Lehrstuhl für Geologie, Fachbereich VI, Geowissenschaften, Universität Trier, D-54286 Trier, Germany*
[b] *Institut für Physische Geographie, Universität Freiburg, Werderring 4, D-79085 Freiburg, Germany*
[c] *Department of Earth Sciences, Simon Fraser University, Burnaby, B.C., Canada V5A 1S6*
[d] *Institut für Umweltgeochemie, Universität Heidelberg, INF 236, D-69120 Heidelberg, Germany*
[e] *Centro de Estudios Cientificos, Valdivia, Chile*
[f] *Instituto Antarctico, Universidad Magallanes, Punta Arenas, Chile*
[g] *Institut für Nachrichtentechnik und Informationselektronik, Universität Rostock, Richard-Wagner-Str. 31, 18119 Rostock, Germany*
[h] *Geologisches Institut, Universität Freiburg, Albertstr. 23A, D-79085 Freiburg, Germany*

Abstract

Late Glacial to Holocene ice retreat was investigated along a 120 km long fjord system, reaching from Gran Campo Nevado (GCN) to Seno Skyring in the southernmost Andes (53°S). The aim was to improve the knowledge on regional and global control on glacier recession with special emphasis on latitudinal shifting of the westerlies. The timing of ice retreat was derived from peat and sediment cores, using mineralogical and chemical characteristics, and pollen as proxies. Stratigraphy was based on ^{14}C-AMS ages and tephrochronology. The ice retreat of the Seno Skyring Glacier lobe is marked by an ice rafted debris layer which was formed around 18,300 to 17,500 cal. yr B.P. Subsequently, fast glacier retreat occurred until around 15,000 to 14,000 cal. yr B.P. during which around 84% of Skyring Glacier were lost. This fast recession was probably also triggered by an increase of the Equilibrium Line Altitude (ELA) from 200 to 300 m. Subsequently, the ice surface was lowered below the ELA in an area that previously made up more than 50% of the accumulation area. Much slower retreat and glacier fluctuations of limited extent in the fjord channel system northeast of GCN occurred between around 14,000 to 11,000 cal. yr B.P. during both the Antarctic Cold Reversal and the Younger Dryas. This slow down of retreat indicates a decline in the general warming trend and/or increased precipitation, due to a southward migration of the westerlies. After 10,100±120 cal. yr B.P. pollen distribution shows evolved Magellanic Rainforest and similar climate as at present, which lasted throughout most of the Holocene. Only Late Neoglacial moraine systems were formed in the period 1220–1460 AD, and subsequently in the 1620s AD, and between 1870 and 1910 AD. The results indicate that the Gran Campo Nevado ice cap has reacted more sensitive and partly distinct to climate change, compared to the Patagonian Ice Field.

Keywords: Andes; deglaciation; palaeo-ecology; glacier balance

1. Introduction

The timing of the Late Pleistocene to Holocene ice retreat and glacier fluctuations along the southern Andes

* Corresponding author. Tel.: +49 651 2014644; fax: +49 651 201 3915.
E-mail address: kilian@uni-trier.de (R. Kilian).

0921-8181/$ - see front matter © 2006 Published by Elsevier B.V.
doi:10.1016/j.gloplacha.2006.11.034

(40°S to 54°S) are still poorly constrained, since on the western side of the Andes moraines or glacial debris were deposited often sub-aquatically and on the Pampean eastern side moraines often do not include suitable material for ^{14}C dating. Mapping of the moraine systems on the continental eastern side of the Andes by e.g. Caldenius (1932) has depicted four major Pleistocene glaciations (Fig. 1 inset). Later additional mapping and ^{14}C radiocarbon dating by e.g. Mercer (1970, 1976), Hollin and Schilling (1981), and Clapperton et al. (1995; Fig. 1) gave first age constraints for moraine building phases. A review of glaciological and palaeo-ecological data by McCulloch et al. (2000) suggested that timing and velocity of ice recession in the Patagonian Andes was regionally diverse. It is also still disputed, if Younger Dryas cooling (12,700 to 11,500 cal. yr B.P: e.g. Goslar et al. 2000 has also affected glaciers of the Patagonian Andes (Lowell et al., 1995; Denton et al., 1999a; Heusser et al., 2000; Hajdas et al., 2003 which would suggest interhemispheric linkage (Bard et al., 1997; Blunier et al., 1998; Steig et al., 1998)).

Based on proxies from a marine sediment core, Lamy et al. (2004) suggested that changes in the Pleistocene extent of the Patagonian Ice Field had a 1000 yr delayed response to changes in Pacific surface water temperatures which are linked with the Antarctic sea ice index. However, glacier extent in the Andes may not only be controlled by temperature, but also by precipitation which may be related to the intensity and shifting of the westerlies (e.g. Heusser, 1989; Labeyrie et al. 2003). Constraints for palaeo-precipitation by lake level reconstructions (e.g. Gilli et al., 2001) or pollen records (McCulloch and Davies, 2001; Moreno et al., 2001; Markgraf et al., 2003 are still scarce for this region and may depict conditions only for local or restricted regional areas. It has to be taken into account that

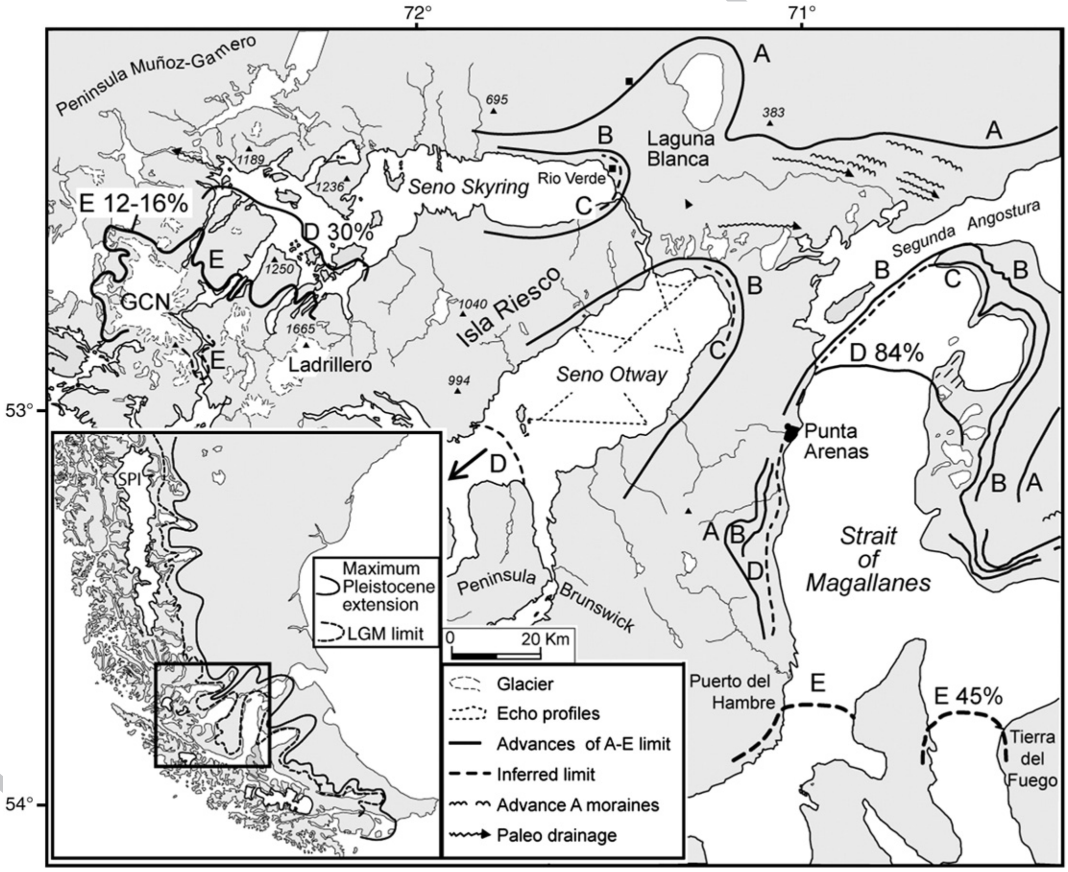

Fig. 1. The inset shows southernmost South America with the present-day extent of the Southern Patagonian Ice Field (SPI), the maximum Pleistocene glacier extent (Caldenius, 1932), and the probable extent during the Late Glacial Maximum (LGM, Lliboutry, 1998). The detailed Andean section between 52°S and 54°S include the investigated area of the Gran Campo Nevado and the Seno Skyring fjord system. Glacial and Late Glacial moraine systems A to E (Clapperton et al., 1995; McCulloch et al., 2000) are shown for Seno Otway and the Strait of Magellan. Possibly related moraine systems D and E are shown for the area of Gran Campo Nevado, Seno Skyring and Seno Otway, and are discussed in the text.

Please cite this article as: Kilian, R. et al. Palaeoecological constraints on late Glacial and Holocene ice retreat in the Southern Andes (53°S). Global and Planetary Change (2006), doi:10.1016/j.gloplacha.2006.11.034

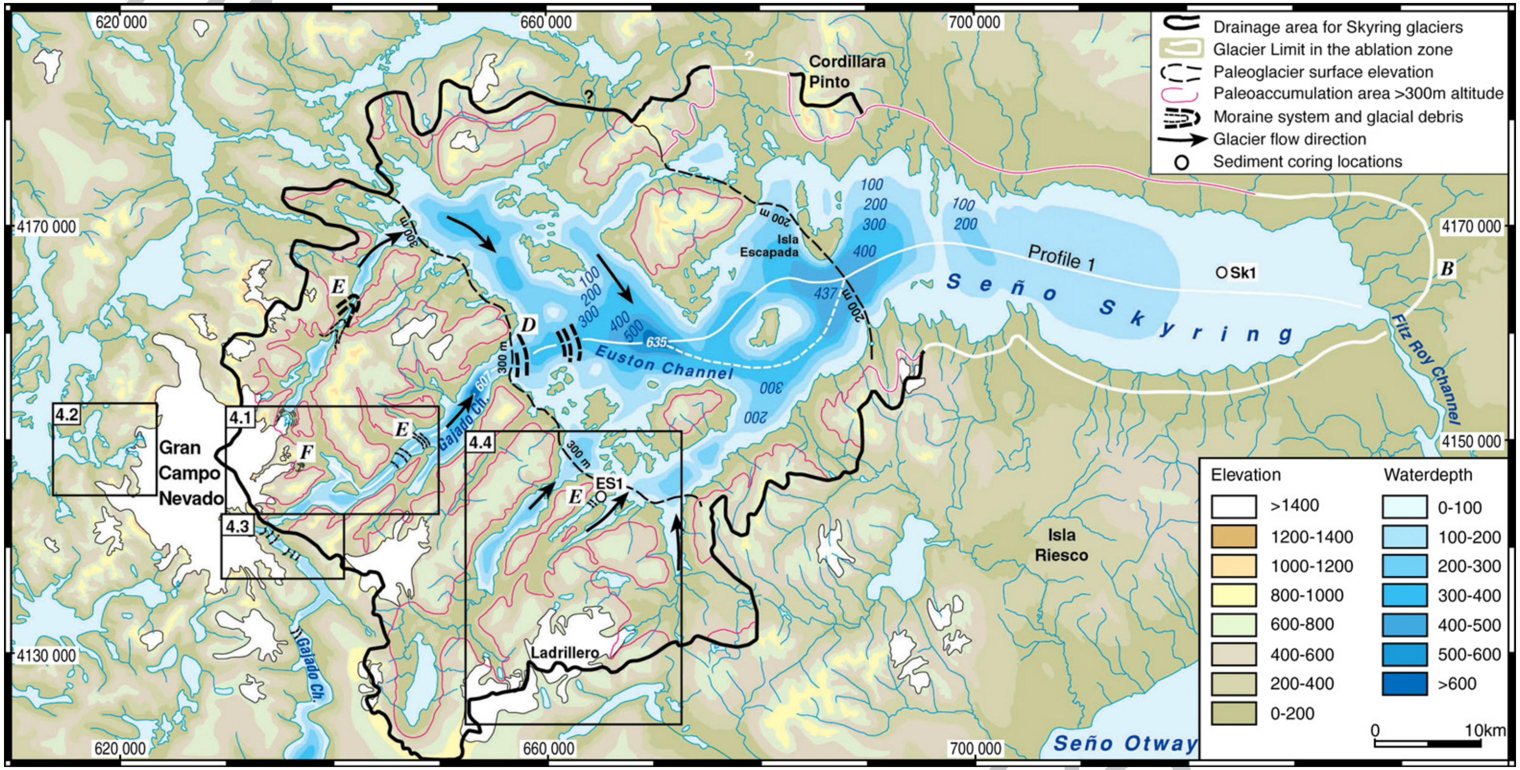

Fig. 2. Topographical and bathymetrical map of Gran Campo Nevado and Seno Skyring area with UTM grid (South American 69). The bathymetry of the fjords and sub-aquatic moraine systems were mapped with echo sounding (Section 2.2) and include data from hydrographical map Nr. 11700 (Senos Otway y Skyring; scale 1:260 000) from Servicio Hidrografico y oceanografico de la Armada de Chile. The topography was adapted from Chilean Topographical Maps 1:100,000 and for the Gran Campo area from Schneider et al. (this issue-a,b). Based on topographical information and field mapping, the palaeo-drainage system of the Skyring Glacier lobe was mapped. The Moraine B system represents the LGM glacier extent (Clapperton et al., 1995) and corresponds to the Rio Verde moraine system (Mercer, 1970, 1976). Further sub-aquatic moraine systems D and E have been mapped by echo sounding (Section 2.2). The location of bathymetrical profile 1 (Fig. 3) is indicated. The Insets 4.1 to 4.4 are presented in Fig. 4.

different localities across the strong climate divide of the Southern Andes (with snow accumulation of up to 13.5 m/yr of water equivalent along the main divide; Godoi et al., 2002) may be affected differently: Stronger westerlies result in higher precipitation near the climate divide of the Andes, but in lower precipitation in the easterly foehn-dominated pre-andean range, and vice versa (e.g. Schneider et al., 2003).

Glacier fluctuations in the Southern Andes do not always clearly reflect changing climate conditions. Especially the velocity of ice retreat may be controlled by glacier bed morphology. In particular depth of lakes or fjords is an important factor controlling glaciers to be grounded or floating (e. g. Pio XI glacier: Rivera et al., 1997; Rivera and Casassa, 1999; O'Higgins glacier: Casassa et al., 1997). Greater depth of proglacial lakes or fjords seems to enhance calving activity in fresh water and even more so in tide water (Warren and Aniya, 1999).

This study tries to constrain the timing and phases of the 120 km long ice retreat from proglacial lake Seno Skyring at 53°S to the small present-day ice cap of Gran Campo Nevado (GCN) in the southernmost Andes. The GCN glacier system may have reacted faster to climate change than the major body of the Patagonian Ice Field (Figs. 1 and 2). An important objective of this study was to determine the sub-aquatic fjord morphology with respect to possible destabilization of glaciers in deep fjord sections and also to detect sub-aquatic moraine systems. Furthermore, palaeoenvironmental implications (e.g. pollen, ice rafted debris, sediment chemistry) were obtained from different sediment and peat cores, collected along the path of the ice retreat. Mapped sub-aquatic moraine systems were related to the sedimentological and palaeo-ecological records to obtain a comprehensive view of the ice retreat phases. Using morphological data and implications on the glacier thickness, changes in the palaeo-accumulation/-ablation areas have been constrained.

2. Materials and methods

2.1. Area of investigation

The Seno Skyring glacier system mainly originates at the Gran Campo Nevado ice cap (GCN) which has a

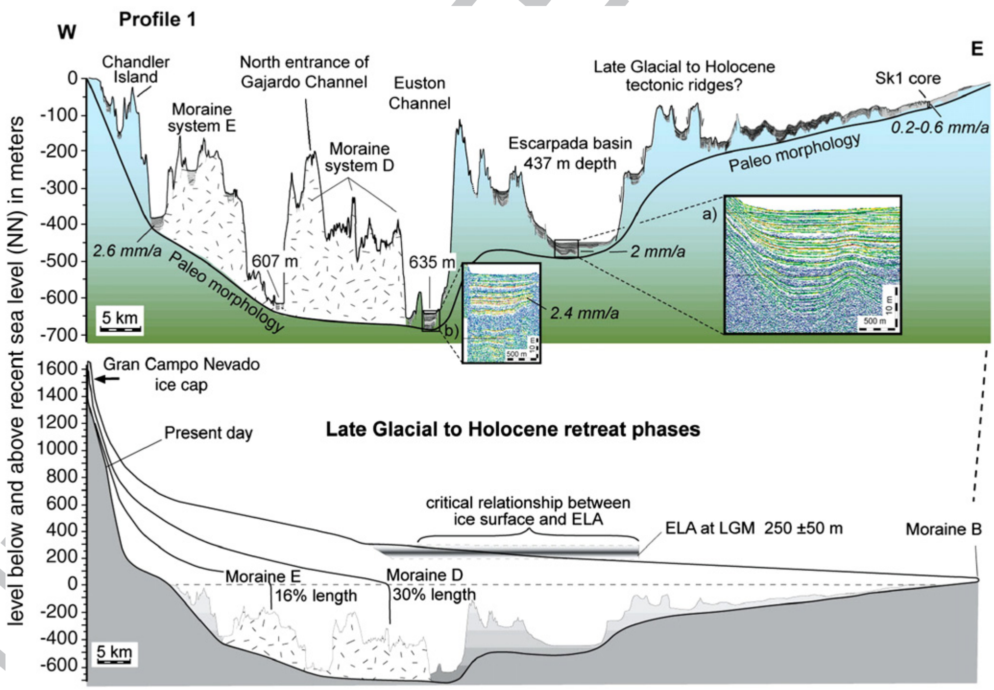

Fig. 3. (Upper): bathymetrical profile 1 (see Fig. 2) of the fjord system from Gran Campo Nevado to eastern Seno Skyring. Moraine D and E limits of the Late Glacial are distinguished (Section 4.1). Sedimentation rates (in italics) along the profile are derived from echo sounding profiles (Section 3.2) and sediment cores (Section 3.3); (lower) The lower profile shows the same bathymetry as in the upper profile and constrains possible palaeo-ice surfaces by field observations (Section 2.2) and the assumption of a slightly logarithmic lowering of the ice surface from the continental ice-divide of Gran Campo Nevado. Different glacial extents for moraine limits B, D and E stages are shown. The loss of glacier length is given relative to the LGM moraine limit B. The insets a) and b) show reflection layers of echo sounding profiles from sedimentary basins (More details in Section 3.2).

Please cite this article as: Kilian, R. et al. Palaeoecological constraints on late Glacial and Holocene ice retreat in the Southern Andes (53°S). Global and Planetary Change (2006), doi:10.1016/j.gloplacha.2006.11.034

maximum elevation of 1750 m and is located at 53°S on the southern Península Muñoz Gamero (PMG), Chile (Fig. 1). At present the GCN ice cap covers an area of 199.5 km^2 (Schneider et al., this issue-a,b). It represents a remnant of a continuous ice field, which during the LGM stretched from the Northern and Southern Patagonian Icefield (NPI and SPI) to the Cordillera Darwin (Fig. 1 inset; Caldenius, 1932; Mercer, 1970; Mercer, 1976). From the Pleistocene ice divide several large glacier systems reached 120 to 200 km towards the east. Ice recession left behind extensive proglacial lake and fjord systems like Seno Skyring, Seno Otway and the Strait of Magellan (Figs. 1, 2).

2.2. Echo sounding, bathymetry and sediment cores

The fjord bathymetry and sediment structures were investigated by a Parametric Echo Sounding System SES 96 from Innomar (Wunderlich and Wendt, 2001; http://www.innomar.com). The SES 96 has a depth range of 0.5 to 800 m with a vertical resolution of <5 cm. Water depths were calculated from the high frequency signal, which was calibrated for measured water temperatures and salinity (http://www.npl.co.uk/acoustics/techguides/soundseawater/content.html). The low frequency signals of the transmitter were chosen between 4 and 12 kHz, trying to get an optimal penetration and resolution for different sediment types. The pulse length was 0.08–1 ms and the beam width ± 1.8°. Sediment depths in echo sounding profiles were calibrated by using five 4–5 m long ^{14}C-dated sediment cores. Penetration was usually between 30 to 50 m. At some local areas sediment penetration was low, probably due to gas formation in organic-rich sediment layers.

Based on echo sounding profiles, representative sediment cores were taken with a 5 m long piston corer (6.5 cm diameter: www.uwitec.au) in fjords and lakes along the transect from GCN to eastern Seno Skyring (Figs. 2–4) with the RV *Gran Campo II* between March 2002 to October 2003. Here we concentrate on three sediment cores, which include the time span from the Late Glacial to the Holocene (Fig. 5). A 4.7 m long core (Sk1) was taken in the eastern section of Seno Skyring in 72 m water depth and >8 km from the nearest shoreline (Fig. 2). The flat slopes of this basin may have precluded turbidites and coarse clastic sediment input. A 4.6 m long core (VO-1) was obtained in 37 m water depth at the north-eastern end of Vogel fjord, an ancient glacial valley originating at Cerro Ladrillero (Fig. 4.4). A 6.4 m long core (CH-1) was taken from a small (70 × 150 m) lake on Chandler Island in the Gajardo Channel (Fig. 4.1).

2.3. Age dating

^{14}C measurements were done by HVEE Tandetron accelerator mass spectrometry (AMS) at Leibniz Laboratory of the University of Kiel, University of Erlangen and Poland (www.radiocarbon.pl). The activity of ^{14}C was determined from acid extracts of terrestrial macrofossils from the sediment cores. In the investigated peat core GC2 (Figs. 4.1 and 6d) plant macrofossils were obtained by sieving 2 g of wet peat through a 1 mm meshed sieve to remove roots and pieces of wood from the peat. ^{14}C-activity was determined in humic acid extracts and also in the humic acid extraction-residues. ^{13}C/^{12}C-ratios were measured simultaneously by AMS and used to correct mass fractionation. Conventional radiocarbon ages and calibrated ages are given in Table 1. All calibrated ^{14}C ages in the text and figures represent mean of one sigma range and has been calibrated with Calpal software (http://wwkw.calpal.de), using the new *Calpal July 2004* calibration curve. It is suggested that this is the best available calibration curve at present, because it considers the most important recent calibrations for different time intervals. Further details are given at http://www.calpal.de and are discussed in Lamy et al. (2004; supporting online material). Cited ^{14}C ages, which were used for comparison, especially in Fig. 8, have also been recalculated with *Calpal 2004* and *Calib 4.4.*

2.4. Chemical analysis

Major and some trace elements (e.g. Sr, Ba, Zr) have been measured by Atomic Absorption Spectrophotometry (AAS; Perkin-Elmer). 100 mg of sediment were dried (105 °C) and were fused in Pt skillets with 400 mg of a flux material (mixture of Lithiumtetraborate, Lithiumcarbonate and Lanthanoxide). Produced glass pearls were dissolved in 40 ml HCl (0.5 N). Liquids of samples and international standards (MRG-1, SY-2 and JG-2) were measured by the AAS. Determined major elements, loss on ignition (1050 °C), and independently detected contents of CO_2 and SO_2 resulted in sums of 99 to 101 wt.%. Carbon and sulphur concentrations were determined by means of a C/S-Analyser (ELEMENTAR) burning 10–20 mg sample aliquots in a tin capsule. Mean relative standard deviations were 2.2% for C and 2.1% for S determinations. Estimated detection limits were 0.01 wt.% for carbon and 0.02 wt.% for sulphur.

2.5. Granulometry

The particle size analyses were made with a Galai CIS-1 laser particle counter with an analytical range

Please cite this article as: Kilian, R. et al. Palaeoecological constraints on late Glacial and Holocene ice retreat in the Southern Andes (53°S). Global and Planetary Change (2006), doi:10.1016/j.gloplacha.2006.11.034

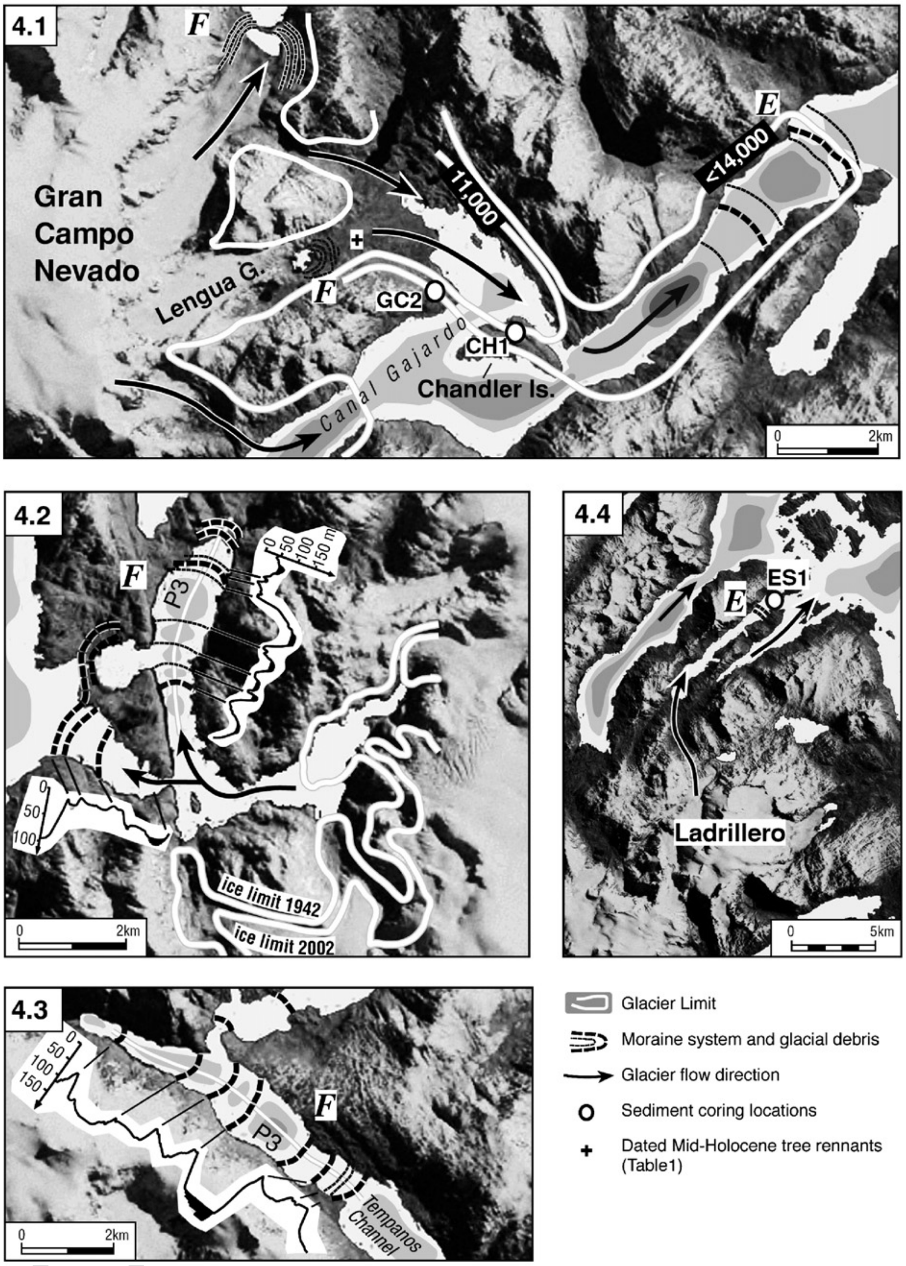

Fig. 4. Local fjord sections (locations see Fig. 2) with moraine systems detected and investigated by bathymetrical surveys. The track of the fjord bottom profiles of 4.1 is shown in Fig. 2. Inset 4.1 shows Gajardo Channel with lake sediment and peat core localities (CH1 and GC2), sub-aquatic moraine systems and constrained moraines/glacier limits D, E and F (details see text). The insets 4.2 and 4.3 show the bathymetrical profiles 2 and 3, which are plotted beside the fjord channels. They show details of sub-aquatic moraine systems which are shown in more detail in Fig. 5. The inset 4.4 shows the location of sediment core VO-1 and its relationship to ancient glacier flows.

between 0.5 and 150 µm. About 50 mg of air-dried sediments were dissolved in 50 ml distilled water. The organic material was removed with a solution of H_2O_2 (10%) over a period of 15 h. Afterwards the samples were placed in 60–70 °C water bath. Finally, the samples were treated in an ultrasound bath for 20 min before being measured with the particle analyzer. The considered ranges of particle sizes are 0.5 to 2 µm (clay), 2 to 63 µm (silt) and 63 to 150 µm (fine sand).

Please cite this article as: Kilian, R. et al. Palaeoecological constraints on late Glacial and Holocene ice retreat in the Southern Andes (53°S). Global and Planetary Change (2006), doi:10.1016/j.gloplacha.2006.11.034

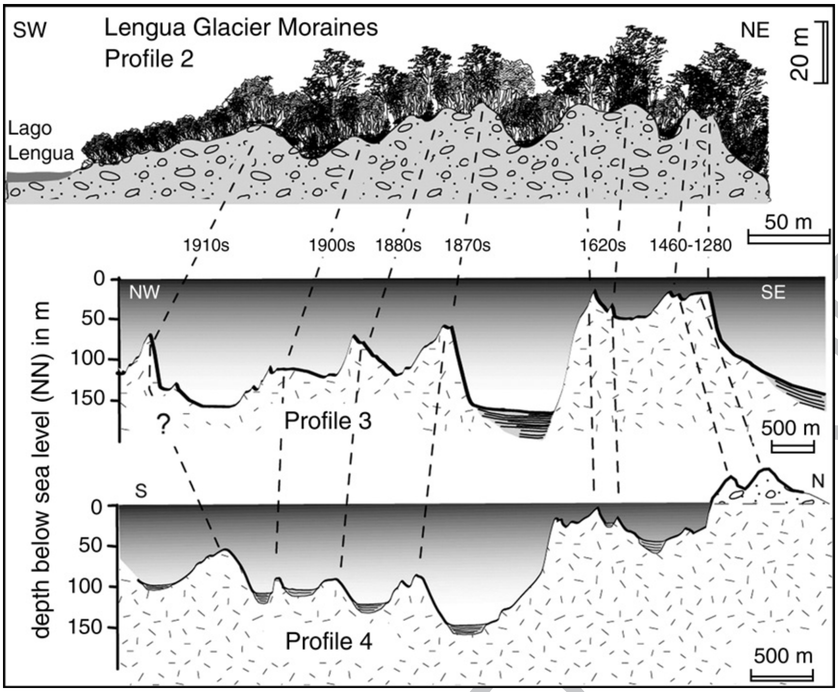

Fig. 5. Comparison of LIA moraine systems of Lengua Glacier (based on dendrochronologically determined ages; location in 4.1; Koch and Kilian, in press) with the bathymetry of sub-aquatic moraine systems in the Tempanos Channel (Fig. 4.2) and the West Glacier Basin (Fig. 4.3), as determined by echo sound profiling.

2.6. Palynology

The 2.9 m long peat to sediment core GC-2 (52° 48′ 37″ S, 72° 55′46″ W) was obtained in proximity to the present-day GCN ice cap (Fig. 4.1). The site is located in a small basin (120 × 80 m) between roche moutonees of the ancient glacial valley in an altitude of about 70 m above sea level. Sampling was done with a Russian corer and for the uppermost 1.8 m of the peat also with a 10 × 10 × 200 cm stainless steel WARDENAAR corer (Wardenaar, 1987). The upper 180 cm consist of peat, which rests on top of 80 cm of glaci-lacustrine sediments (Fig. 6d). Chemical and mineralogical characteristics are described by Franzen et al. (2004). Samples for pollen were collected from 2 cm cuts of the core. Due to ^{14}C dating each sample represents less than 200 yr (Fesq-Martin et al., in press). The samples were processed using standard techniques (e.g. Faegri and Iversen, 1989). Exotic spores (*Lycopodium*) were added to calculate pollen concentrations. Frequencies (%) of trees, shrubs and herbs typically added up to terrestrial pollen sums of 400–900 grains. Further information on pollen identification, pollen of aquatic plants, spores, and ecological implications for the evolution of the Magellanic Rainforest are given by Fesq-Martin et al. (in press). Here we concentrate on selected pollen with implications for palaeo-climate and extend of glaciation.

3. Results

3.1. Morphology and bathymetry

Glacier flow direction and thickness of glaciers flowing from the Gran Campo Nevado ice cap towards Seno Skyring (Fig. 2) were constrained by field observations of striations on basement rocks, fjord morphology and the elevation at which erratic blocks were found. In the Skyring drainage area (Fig. 2) glaciers of Gran Campo Nevado and Cerro Ladrillero followed 10–25 km long, NE-striking fjords, which have been eroded along dextral transform faults (Fischbach et al., 2001). These 3 to 7 km wide fjords converge in the Euston Channel where the glaciers turned east. The palaeo-drainage system of Skyring Glacier was mapped in Fig. 2 within a South American 69-UTM grid by field observations, a Landsat TM 5 scene, Shuttle Radar Topography Mission data (http://srtm.usgs.gov), topographical maps (Carta Aeronautica, SAF 1:250 000) and aerial photos of the region around Gran Campo Nevado (Schneider et al., this issue-a,b).

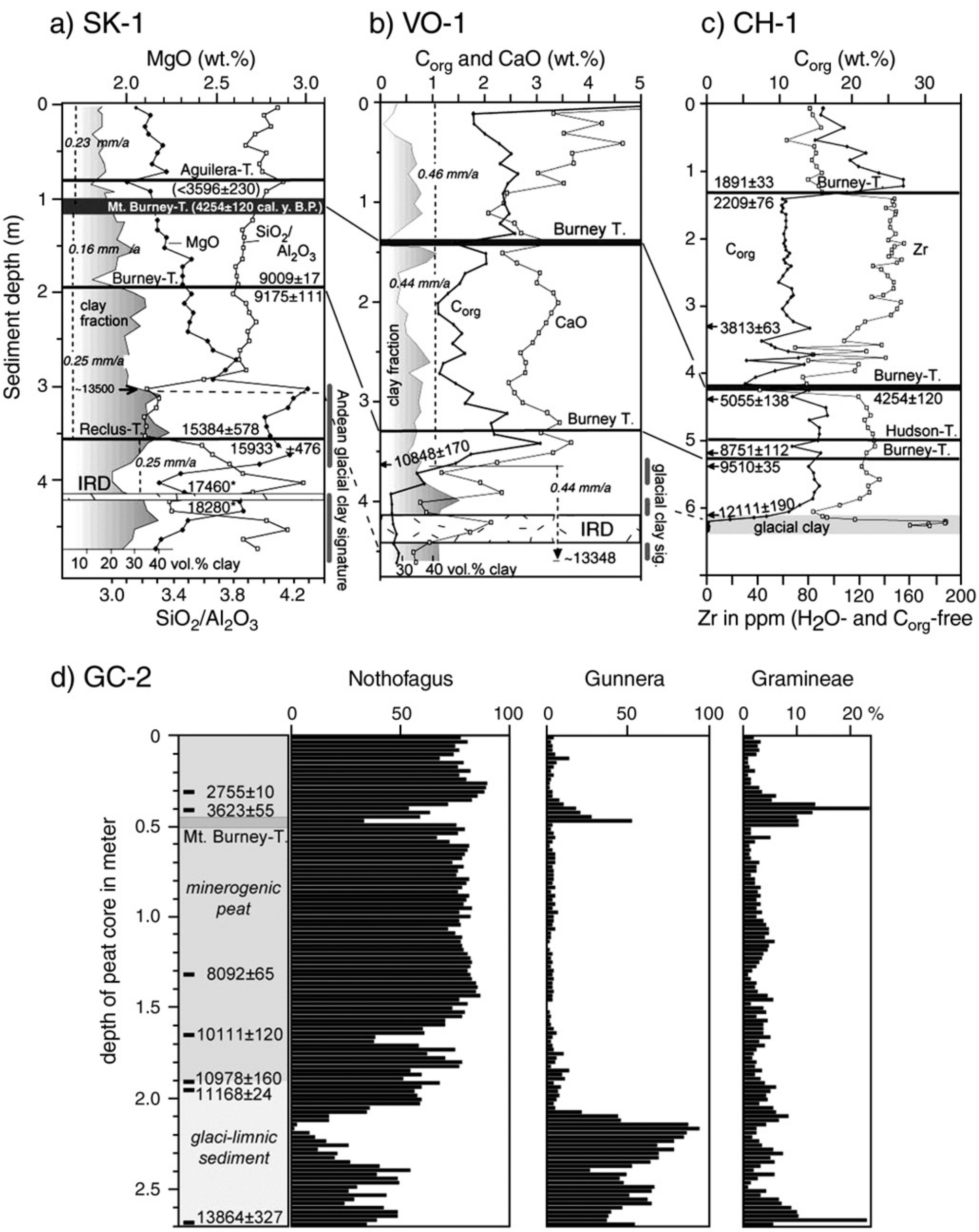

Fig. 6. Depth profiles of sediment and peat cores from the Seno Skyring and Gran Campo Nevado area with tephra layers (minimum and maximum ages after Kilian et al., 2003) and ^{14}C ages in cal yr B.P (Table 1 and Section 2.3). Sedimentation rates for certain core sections are given in italic numbers. a) Sediment core SK-1 (eastern Skyring, Fig. 2) includes chemical pattern (C_{org}, MgO, SiO_2/Al_2O_3 ratios), volume% of clay fraction (>63 um), and ice rafted debris layer (IRD; with lithic grains >2 mm); b) Sediment core VO-1 (south-western Skyring area, Figs. 2 and 4.4) is shown with C_{org} and CaO contents, volume % of clay fraction and IRD layer; c) CH-1 core from a lake on Chandler Island (Locality in Fig. 4.1) include C_{org} and Zr contents, and a layer of glacial clay; d) Peat core GC-2 from the Bahia Bahamondes area, northeast of Gran Campo Nevado (Locality in Fig. 4.1) with lithological characteristics (minerogenic and glaci-limnic) and % diagram of the terrestrial *Nothofagus, Gunnera* and *Graminae* pollen (Fesq-Martin et al., in press).

Echo sounding profiles of a total length of 560 km were obtained from the Skyring fjord system. The bathymetry of Fig. 2 was obtained from longitudinal echo sounding profiles of the fjords (Figs. 3, 4), completed by perpendicular and zigzag echo sounding profiles and are compiled together with water depth information from hydrographical map Nr. 11700 (Senos Otway y Skyring; scale 1:260 000) from Servicio

Please cite this article as: Kilian, R. et al. Palaeoecological constraints on late Glacial and Holocene ice retreat in the Southern Andes (53°S). Global and Planetary Change (2006), doi:10.1016/j.gloplacha.2006.11.034

Table 1
AMS ^{14}C ages with calibrations after *CALIB 4.4* and *CALPAL*, used for age constraints in peat and sediment cores and a mortified Mid-Holocene tree remnant

Core	Core depth cm	Submitted material	^{14}C age	cal BP age ranges (1 sigma)[a]	Calibrated yr BP[b] (1 sigma)	Laboratory	Reference
CH-1	337	Macro rest >5 mg C	3545±35	3727–3747, 3762–3791, 3825–3873, 3877–3887	3813±63	Poland[c]	this paper
CH-1	422	Macro rest 1.6 mg C	4420±40	4873–4934, 4958–5047, 5194–5205	5055±138	Kiel[d]	Kilian et al. (2003)
CH-1	520	Macro rest 4.8 mg C	7890±45	8599–8724, 8727–8769, 8833–8844, 8922–8927	8751±112	Kiel[d]	Kilian et al. (2003)
CH-1	536	Macro rest 0.6 mg C	8520±70	9471–9548	9510±35	Kiel[d]	Kilian et al. (2003)
CH-1	605	Macro rest 2.9 mg C	10320±55	11781–11788, 11946–12340, 12549–12556	12111±190	Kiel[d]	Kilian et al. (2003)
GC-2	31	Macro rest >3 mg C	2620±30	2742 - 2765	2755±10	Kiel[d]	Fesq-Martin et al. (in press)
GC-2	41	Macro rest >3 mg C	3382±44	3569–3650, 3654–3688	3623±55	Erlangen[e]	Fesq-Martin et al. (in press)
GC-2	133	Macro rest >3 mg C	7288±67	8026–8099, 8105–8167	8092±65	Erlangen[e]	Fesq-Martin et al. (in press)
GC-2	165	Macro rest >2 mg C	9024±80	9921–9933, 9958–9993, 10011–10017, 10031–10055, 10069–10078, 10112–10135, 10146–10242, 10353–10354	10111±120	Erlangen[e]	Fesq-Martin et al. (in press)
GC-2	191	Macro rest >2 mg C	9659±83	10786–10829, 10842–10943, 11012–11015, 11062–11175	10978±160	Erlangen[e]	Fesq-Martin et al. (in press)
GC-2	195	Macro rest 4.3 mg C	9740±42	11140–11149, 11155–11200	11168±24	Kiel[d]	Fesq-Martin et al. (in press)
GC-2	269	Macro rest 0.3 mg C	12017±203	13544–13734, 13787–14330, 14861–14936	13865±327	Kiel[d]	Fesq-Martin et al. (in press)
VO-1	365	Macro rest >3 mg C	9490±50	10600–10608, 10640–10656, 10671–10766, 10833–10836, 10958–11005, 11017–11059	10848±170	Poland[c]	this paper
GCN-02-GB		Tree remnant 4.3 mg C	4719±49	5327–5383, 5394–5396, 5449–5485, 5529–5578	5455±99	Kiel[d]	this paper

[a] Ages calibrated with CALIB REV 4.4.2 and database intcal 98 (Stuiver and Reimer, 1993, Radiocarbon, 35, 215–230).
[b] Ages calibrated with CALPAL and the calibration curve CalPal2004_SFCP.
[c] Poznan Radiocarbon Laboratory, Poland.
[d] Leibniz Labor für Altersbestimmung und Isotopenforschung Christian-Albrechts-Universität Kiel.
[e] Physikalisches Institut der Universität Erlangen-Nürnberg.

Hidrografico y oceanografico de la Armada de Chile (SHOA). In addition, profiles were obtained from the relatively shallow (<220 m) eastern section of Seno Otway (Fig. 1), where no sub-aquatic moraine systems have been detected.

Along the Skyring fjord system the greatest depths occur in Euston Channel (635 m water depth; Figs. 2 and 3) and in the northern entrance of Gajardo Channel (607 m water depth). This is a significantly smaller glacial overdeepening than in the western Strait of Magellan (~1130 m water depth; Hydrographical Map Nr. 11000 with scale 1:1,000,000 from SHOA) and Baker Fjord (1344 m water depth) between SPI and NPI. Longitudinal Profile 1 (Figs. 2 and 3) illustrates the bathymetry and sediment structures along the glacier pathway from the Late Glacial ice divide at Gran Campo Nevado towards Seno Skyring. The greatest water depths occur in the central and western drainage system (Fig. 3). Mapping of fjord morphology and erratic blocks along the Euston Channel (Fig. 2) indicate that the maximum valley glacier surface did not exceed around 400 m present-day elevation. Together with the fjord bathymetry this indicates that the ice sheet may have reached around 900 to 1000 m thickness in the western Skyring section and implies that the glacier was grounded (Fig. 3, lower profile). This ice thickness is much smaller than proposed for the SPI during the LGM (up to 2700 m ice thickness: e.g. Hulton et al., 1994). Large water depths occur also in sections where morphology and bathymetry indicate that glacier flow

Please cite this article as: Kilian, R. et al. Palaeoecological constraints on late Glacial and Holocene ice retreat in the Southern Andes (53°S). Global and Planetary Change (2006), doi:10.1016/j.gloplacha.2006.11.034

was constricted (e.g. in a 437 m deep basin to the south of Escarpada Island (Fig. 2), probably due to the narrowing of the glacial valley which leads to higher flow velocity and successively higher erosion rates at the basis of the glacier.

Profile 1 of Fig. 3 shows several sub-aquatic ridges, which occur perpendicular to the palaeo-glacier flow direction (Fig. 2), mainly in Gajardo Channel (Fig. 4.1). In fjords around Gran Campo Nevado these sub-aquatic ridges are interpreted as moraine systems, if no relationship to on-land geomorphology or tectonic ridges are recognized (Figs. 4.1 and 5). With the exception of the Tempanos fjord section of Gajardo Channel (Fig. 4.2) there are no moraine remnants above sea or lake level on the steep fjord slopes. To the east of Euston Channel and in Seno Skyring no moraine ridges were found. Several sub-aquatic ridges were found across the middle section of Seno Skyring from north to south with less than 100 m water depth (Figs. 2, 3). These ridges can be traced to Neogene faults and thrusts that are found on land nearby (Fischbach et al., 2001; Lodolo et al., 2002; Fig. 2). Some of these ridges are so prominent that we suggest that they were still active during the Late Glacial and/or the Holocene or that they could represent vertical displacements related to glacial rebound of the Andes.

3.2. Sediment echo sounding

Sediment echo sounding profiles in eastern Seno Skyring show 5 to 10 m of fine-grained well-sorted sediments with sharp reflectors on top of coarse clastic and unsorted glacial detritus which were identified in sediment core SK-1 (Section 3.3) as ice rafted debris (IRD). Below the IRD reflector only little sediment (<1 m) was deposited above another reflector, which did not enable further penetration for the echo sound. We interpret basal reflector as the older consolidated, probably Tertiary, sedimentary basement. Assuming that the upper 5 to 10 m thick sediment layer was deposited during the last 17,500 yr (compare results of SK-1 sediment core in Fig. 6a and Section 3.3), the Late Glacial and Holocene sedimentation rates have varied between 0.3 to 0.6 mm/yr in this proglacial lake section.

In the 437 m deep basin to the south of Escarpada Island in central Seno Skyring (Fig. 2) the sediment echogram shows around 30 m of fine-grained and well-sorted Late Glacial and Holocene sediments on top of the basement (Figs. 3, inset a). Assuming deposition during the last 16,000 yr after ice retreat (Section 4, Discussion), this suggests even higher sedimentation rates of ~2 mm/yr.

Further to the west, where annual precipitation is greater than 2500 mm/yr (Schneider et al., 2003), echograms from the 635 m deep basin in the Euston channel (Fig. 3, inset b) show 36 m of fine-grained and well-sorted Late Glacial and Holocene sediments. The ice retreat from Euston Channel (Fig. 2) was constrained between around 16,500 and 14,000 cal. yr B.P. (Discussion on timing ice retreat in Section 4.1). Assuming a deposition during the last 15,000 yr after the ice retreat, the sedimentation rates amount to 2.4 mm/yr. In basins between moraine E ridges in the Gajardo Channel (Figs. 2, 3 and 4.1) echograms show up to 37 m of fine-grained clayey sediments. Assuming an ice retreat from this area after around 14,000 cal. yr B.P. (Sections 3.3 and 4.1), calculated sedimentation rates were in excess to 2.6 mm/yr. This can be explained by high annual precipitation in excess to 6500 mm/yr (Schneider et al., 2003) and the input of glacial clay from the Holocene outlet glaciers of GCN (Schneider et al., this issue-a,b).

3.3. Sediment records

The clayey to silty SK-1 sediment core (Figs. 2, 6a) from eastern Seno Skyring does not contain macro plant remnants or biogenic carbonate for ^{14}C determination. Organic carbon content is lower than 1.5 wt.% and was considered as not suitable for ^{14}C dating. However, tephra layers from volcanoes of the Austral Andes Volcanic Zone (AVZ) can be identified by their geochemical fingerprint (Stern, 1990). ICP-MS trace element data (analysed at Act-Labs: www.actlabs.com) were obtained for glass fractions of each tephra layer. The Sr/Y, La/Yb and Zr/Hf ratios were used to distinguish products of the AVZ volcanoes Aguilera, Burney and Reclus (Stern and Kilian, 1996). Age constraints for these tephra layers have been given specifically for the Strait of Magellan and Skyring area by Kilian et al. (2003). In the SK-1 core an Aguilera tephra was identified in 82–84 cm depth (<3596± 230 cal. yr B.P; Fig. 6a; Kilian et al., 2003), a prominent tephra of Mt. Burney was detected in 102 to 108 cm depth (4254±120 cal. yr B.P.; McCulloch and Davies, 2001; Kilian et al., 2003), another early Holocene Mt. Burney layer was at 192–195 cm depth (minimum of 9009±17 and maximum of 9175±111 cal. yr B.P.; Kilian et al., 2003) and a layer of Reclus volcano was found in 356–358 cm depth (minimum of 15,380±578 and maximum of 15,930±476 cal. yr B.P.; Kilian et al., 2003). These age constraints indicate relatively low sedimentation rates between 0.16 and 0.26 mm/yr, with the lowest rates of 0.16 mm/a during the Holocene climate optimum between 9000 and around 4500 yr ago (Fig. 6a, 7f and Section 4). An IRD layer with lithic grains >2 mm was found at 420 cm core depth. Assuming sedimentation

Please cite this article as: Kilian, R. et al. Palaeoecological constraints on late Glacial and Holocene ice retreat in the Southern Andes (53°S). Global and Planetary Change (2006), doi:10.1016/j.gloplacha.2006.11.034

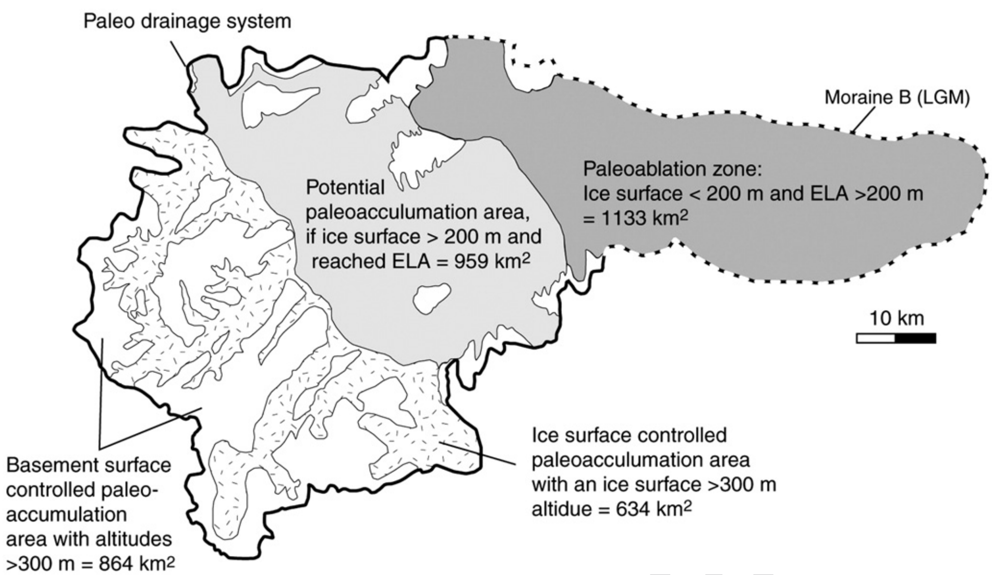

Fig. 7. The distribution of the Skyring Glacier system during the LGM with probable palaeo-accumulation and ablation areas, which have been calculated with ArcGis 8.0. Details of the mapped areas can be seen in Fig. 2.

rates of 0.25 mm/a below the Reclus tephra layer (Fig. 6a), the IRD layer was formed between 17,460 and 18,280 cal. yr (±500 yr).

The volume % of clay fraction (0.5 to 2 µm) is positively correlated with MgO content and negatively with SiO_2/Al_2O_3 ratios (Fig. 6a). Between around 16,000 to 13,500 cal. yr B.P., relatively high amounts of clay fraction and MgO contents indicate a chlorite-rich sediment transport from mafic lithologies (Rocas Verdes formation: Mapa Geologica de Chile 2003; 1:1 000 000) of the Andes (Gran Campo Nevado and to the north) towards the coring site in eastern Seno Skyring (Fig. 2). This may indicate a still extended glaciation in the Cordillera for that period. Since around 13,500 cal. yr B.P. this Andean glacial-clay signature decreases at first rapidly and than more slowly (Fig. 6a), probably due to glacier retreat and establishment of vegetation and soils.

The clayey to silty VO-1 sediment core (Figs. 2, 4.4, 6b) includes the tephra layer of Mt. Burney (4254±120 cal. yr B.P.; McCulloch and Davies, 2001; Kilian et al., 2003) at 138–142 cm depth. The second early Holocene tephra layer (minimum of 9009±17 and maximum of 9175±111 cal. yr B.P.; Kilian et al., 2003) was identified at 332 cm depth. Leaves, found at 365 cm depth, gave a ^{14}C age of 10,848±170 cal. yr B.P (Table 1). This age marks a rapid increase of C_{org} content from 0.5 to 3 wt.%. This value remains relatively high throughout the Holocene, indicating establishment of Magellanic Rainforest. At the same time the relatively high volume % of Late Glacial clay fraction (40–45 vol.%) change to lower values of Holocene clay fractions (25–35 vol.%; Fig. 6b). After 10,848±170 cal. yr B.P and throughout the Holocene sediments have significantly higher CaO contents (2–5 wt.%) than during the Late Glacial (0.5–2.2 wt% CaO). Since biogenic carbonate is absent, we suggest for the Late Glacial a higher contribution of glacial clay from a more remote Ca-poor source (Cerro Ladrillero; Figs. 2 and 4.4), whereas the Holocene sedimentation was controlled by local terrigenous and organic sources. Sedimentation rates of 0.46 and 0.44 mm/a are also nearly constant throughout the Holocene (Fig. 6b). Assuming the same sedimentation rates for the Late Glacial, the base of the core at 465 cm would correspond to approx. 13,300 cal. yr B.P. and a coarse grained IRD layer between 415 and 443 cm would have been deposited around 13,000 yr ago.

The 6.5 m long sediment core CH-1 from a 16 m deep lake on Chandler Island in Gajardo Channel (Figs. 2 and 4.1) was dated by five AMS ^{14}C ages from macro plant remnants (Table 1; Fig. 6c). The sediment core includes also four tephra layers, which are used for further chronological control (Kilian et al., 2003). A glacial clay forming the base of the core has distinct chemical pattern (e.g. high Zr contents) compared to Holocene sediments formed later, suggesting an allochthonous origin of this clay (Fig. 6c). Above the clay the C_{org} content increases to >10 wt. % (Fig. 6c), indicating retreat of the glacier from the island towards the west and

Please cite this article as: Kilian, R. et al. Palaeoecological constraints on late Glacial and Holocene ice retreat in the Southern Andes (53°S). Global and Planetary Change (2006), doi:10.1016/j.gloplacha.2006.11.034

northwest, and the start of soil development and vegetation colonisation on Chandler Island (Fig. 4.1). A ^{14}C date of 12,110±190 cal. yr B.P. marks this rapid change to biogenic sedimentation and glacier retreat from the Chandler Island. The Holocene record of CH-1 shows high C_{org} contents and higher sediment accumulation after the Mt. Burney eruption (4254 cal. yr B.P.), which we interpret as a result of tephra rework rather than a climatic signal (Kilian et al., 2003).

3.4. Pollen record

The 269 cm long core GC 2 (Locality in Figs. 4.1 and 6b) has been dated by seven AMS ^{14}C-ages (Table 1; Franzen et al., 2004; Fesq-Martin et al., in press) and tephrachronology (Kilian et al., 2003). Details of the pollen spectrum are given by Fesq-Martin et al. (in press). Sedimentation and pollen deposition at this site could not have started before significant recession of the glacier in Gajardo Channel (Fig. 4.1.). Between 13,860±327 and 11,170±24 cal. yr B.P. the pollen record is characterized by the species-poor association of the pioneer plant *Gunnera magellanica* together with *Cyperacea* and *Nothofagus* which sum up to >90% of all terrestrial pollen. This is the typical present-day plant association for well-drained moraines and glacial debris near glacier limits. The likely lateral glacier extent below the GC2 is shown in Fig. 4.1 for this time interval. Considering inclination of >5° for the glacier surface in flow direction, the glacier could not have reached further into Gajardo Channel than moraine E limit. From 10,110±120 cal. yr B.P. until at least the mid-Holocene, the palynological record shows a plant association that is typical for an evolved Magellanic Rainforest (climax stage). This indicates temperate and humid conditions comparable to present-day conditions throughout the early to mid-Holocene. Only after the eruption of Mt. Burney (4250 cal. yr B.P.; Kilian et al., 2003) the palynological record (Fig. 6d) shows disturbances, which are more likely related to tephra deposition with associated sediment rework than climate fluctuations.

3.5. Constraints on palaeo-accumulation and ablation areas

The accumulation area ratio (AAR) of mid-latitude glaciers is usually around 0.6. Most Patagonian glaciers have higher ratios of 0.7 to 0.8, since the ablation area is reduced due to iceberg calving in tidewater (Aniya et al., 1996). Glaciers, which are in negative disequilibrium with the present-day climate, may also have low AAR's of 0.4 (Schneider et al., this issue-a,b). The morphology and bathymetry of the Skyring fjord system (Fig. 2) and the estimated palaeo-glacier thickness (Fig. 3) suggest that the Skyring glacier was mostly grounded. However, during glacier recession, iceberg calving could have increased the AAR.

In the period of 2000 to 2003 the Lengua Glacier, an outlet glacier of the GCN ice cap, had varying Equilibrium Lines Altitudes (ELAs) ranging from 650 m to 760 m (Schneider et al., this issue-a,b). During the LGM an ELA depression of around 400 m has been suggested for this Andean area (Hollin and Schilling 1981; Clapperton et al., 1995). Andean foothills north of Seno Skyring reaching elevations of 350 to 200 m do not show any morphological evidence for a glaciation during the LGM. Therefore we assume LGM ELA's at an elevation of 200 to 300 m.

During LGM moraine stage B (Fig. 2) Skyring Glacier covered an area of ~3600 km^2 (Fig. 7). Only ~860 km^2 or ~930 km^2 of the Skyring watershed lie above 300 m or 200 m respectively. This leads to very low AAR's of 0.24 to 0.26, if an ELA of 200 to 300 m above sea level is assumed. Such a low AAR preclude that the Skyring Glacier reached the moraine B limit (Figs. 2 and 7). High accumulation rates in the southern Andes due to either strong westerly winds or due to higher humidity during the early stages of the last glaciation may have depressed the ELA in the Andes so much that the ice surface of valley glaciers protruded above the ELA. If we assume that the surface of the valley glaciers in the south-western part of the Skyring watershed reached the ELA (~630 km^2: Fig. 7), the AAR was 0.42. This value is still too low to have the glacier system reach the moraine B limit (Fig. 2). If we assume an ELA of 200 m and a palaeo-valley glacier surface above 200 m in the section west of Escarpada Island (Figs. 2 and 7), an additional 960 km^2 of glacier surface area would have been part of the accumulation zone. This scenario would have increased the AAR to 0.68. These considerations suggest that the ice surface reached above the ELA in the fjords northeast of GCN and partly in the Euston Channel region (Figs. 2 and 7).

Based on field observation in area of the Euston channel, the Fig. 3 (lower profile) indicates that the slope of the glacier was very low (<5‰) in the Euston Channel area. Therefore this area would have been very sensitive to changes in the ELA. Due to the critical relationship between the elevation of the ice surface and the ELA in the Euston region, small-scale climatic changes could have resulted in dramatic changes of the glacier mass balance. This could explain the dramatic retreat of Skyring glacier (loss of around 80–90% glacier length) between around 17,500 and 14,000 cal. yr B.P., as discussed in the following Section 4.1.

Please cite this article as: Kilian, R. et al. Palaeoecological constraints on late Glacial and Holocene ice retreat in the Southern Andes (53°S). Global and Planetary Change (2006), doi:10.1016/j.gloplacha.2006.11.034

4. Discussion

4.1. Glacier retreat phases

Regional glacier retreat phases with moraine systems A to E (Figs. 1 and 2) have been proposed for the Late Glacial in the Strait of Magellan region by Clapperton et al. (1995) and are discussed in the context of our new results:

4.1.1. Moraine limit A

Due to missing organic material and ^{14}C dates it is still disputed how far east Skyring Glacier reached during the last glaciation. It is possible that this glacier reached as far as Laguna Blanca, corresponding to the moraine limit 3 of Caldenius (1932; Fig. 1 inset), which is identical with the moraine A limit of Clapperton et al. (1995). For this most extended moraine A limit no confining ages exist.

4.1.2. Moraine limits B and C

The moraine limit B (Figs. 1 and 2) corresponds to the moraine limit 4 of Caldenius (1932) and to the Rio Verde moraines which were described along the eastern shore of Seno Skyring by Mercer (1970). The retreat from moraine limit A to B may be due to worldwide dryer conditions at the LGM (e.g. Blunier et al., 1998) or less westerly influence in this area (Lamy et al., 1998, 1999). Reported ^{14}C minimum ages for the moraine limit B along the Strait of Magellan date are 16,800 cal yr B.P. (Clapperton et al., 1995) and 17,150 cal. yr B.P. (McCulloch et al., 2000). At approximately the same time(around 17,400 cal. yr B.P.) the end of full glacial climate conditions was determined for the Chilean Lake district (Lowell et al., 1995; Denton et al., 1999b).

The LGM moraine limit B of Seno Otway and Strait of Magellan were probably formed at the same time than moraines around the eastern shore of Seno Skyring (Fig. 1; Mercer, 1976; Clapperton et al., 1995). The minimum ages of around 17,000 cal. yr B.P. for the initiation of the recession of Skyring Glacier from the moraine limit B by the former authors (Figs. 2 and 3) is in good agreement with the deposition of ice rafted debris, for which we have estimated an age of 17,460 to 18,280 cal. yr B.P. (Skyring sediment core SK-1 in Fig. 6a and details in Section 3.3). The moraine system C, which was described for the Strait of Magellan by Clapperton et al. (1995), is not preserved or yet detected along the eastern shore of Seno Skyring and Seno Otway.

4.1.3. Moraine system D

Clapperton et al. (1995) has mapped a further moraine system D in the Strait of Magellan. Its age was constrained by a clustering of several ^{14}C minimum ages at around ~16,000–17,600 cal. yr B.P. (Clapperton et al., 1995). Moraine limit D appears at 84% glacier length compared to moraine limit B of the LGM (Fig. 1). No comparable moraine systems have been detected between the eastern shore line of Seno Skyring and the south-western region of Euston Channel, where extensive sub-aquatic moraines were detected (Figs. 2 and 3). Although the moraines of Euston Channel are undated and do only represent 30% glacier length compared to LGM, we suggest that they formed coeval to the moraine limit D of the Strait of Magellan, since the IRD layers in the Eastern Skyring are only small and were formed between 17,460 to 18,280 cal. yr. B.P., only some decades before the formation of moraine system D in the Strait of Magellan (details in Section 3.3). Parts of this fast retreat from moraine limit B to D occurred in a lake section with water depths of >600 m (Fig. 3) which most likely enhanced glacier recession by iceberg calving and freshwater circulating below the partially floating snout of the glacier (Warren and Aniya, 1999). Echo sounding profiles also do not show sub-aquatic moraines between the north-eastern shoreline of Seno Otway and the small islands in the south-western section of Seno Otway (Fig. 1). This indicates that in Seno Otway the moraine stage D was also formed closer to the Andes (Fig. 1).

During glacier retreat from moraine system B to moraine system D, the proglacial lakes of Seno Skyring and Seno Otway were connected by Fitz Roy Channel (Figs. 1 and 2, Mercer, 1970) and water of both lakes drained towards the Atlantic (Fig. 1). This kept the lake level relatively constant at around 22–25 m above present-day sea level and lead to the formation of erosional terraces by wave erosion along the lakeshores exposed to the westerlies. A basal peat in the former spillway of Seno Otway to the Atlantic was dated by Mercer (1970) to 14,599±446 cal. yr B.P. (12,460±190 ^{14}C yr). This postdates the deglaciation of Jerónimo Channel (Western entrance of Seno Otway), which led to opening of a fjord-connection to the Pacific (Fig. 1). This age also marks a further glacier recession towards moraine limit E (Figs. 1 and 2).

4.1.4. Moraine limit E

Around 20 km southwest of the moraine system D in Euston Channel, a further sub-aquatic moraine system was formed in the Gajardo Channel (Figs. 2 and 4.1). Pioneer plants, which typically grow on well-drained glacial debris, are recorded in the peat Core GC2 between 13,864±327 and 11,168±24 cal. yr B.P. They are indicating the presence of a glacier in the fjord valley below this site (Section 3.4). Assuming that at this site located 70 m a.s.l. the glacier surface had an inclination of 5–10‰ towards the north-eastern Gajardo Channel (Figs. 3b and 4.1), it is obvious that the glacier could not have reached further than to the observed sub-aquatic moraine system E in the central section of the north-western Gajardo Channel (Fig. 4.1). The ice retreat from Chandler Island (Fig. 4.1) is also traced by the change in sedimentation from glacial clay to organic peat-rich sediment at 12,111 ± 190 cal. yr B.P. (Fig. 6c). This period between 14,000 and 11,000 cal. yr B.P. corresponds with a certain delay to that of the moraine limit E in the Strait of Magellan, which represents an extensive, 80 km long Late Glacial glacier advance dated by ^{14}C ages between 15,350 to 12,250 cal. yr B.P. (Clapperton et al., 1995; McCulloch et al., 2000). While moraine limit E in the Strait of Magellan represent 45% glacier length compared to the LGM moraine B limit, the related moraine limit E in Gajardo Channel represents only 16% glacier length compared to the moraine limit B.

4.1.5. Moraine limit F

The palynological record of GC-2 peat core (Fig. 6d; Section 3.4) indicates a climate optimum after 10,110 ± 120 cal. yr B.P. until at least the eruption and deposition of tephra from the Mt. Burney volcano at 4250 cal. yr B.P. (Kilian et al., 2003). No sub-aquatic or terrestrial moraine systems have been detected between Chandler Island and the moraine belt of Lengua Glacier, which situated 8 km to the west-northwest. These moraines were formed during the Little Ice Age (Koch and Kilian, in press) and are termed moraine limit F (Fig. 4.1). 2 km east of moraine limit F soils and fluvial sediments are deposited on top of mortified tree trunks, which have been dated to 5460 ± 99 cal. yr B.P. (Locality marked by a cross in Fig. 4.1.; Table 1). This indicates that there was no glacier advance beyond LIA moraine Limit F at least during the last 5500 yr. In contrast, Hodell et al. (2001) found Neoglacial conditions with IRD deposition for the South Atlantic after around 5500 cal. yr B.P. (Fig. 8g). Mercer (1970, 1982) and Porter (2000) have also reported significant Neoglacial advances between 5400 and 4500, 3500 and 2400 and around 1500 cal. yr B.P. for several glaciers of the Andes between 40°S to 51°S (e.g. Tyndall, Upsala, Ameghino, Frias, Moreno, Rio Manga Norte and Témpano Glacier; Mercer, 1970, 1976; Aniya, 1995, 1996; Porter, 2000).

LIA moraine systems have been studied in detail with dendroecological methods (Koch and Kilian, in press)

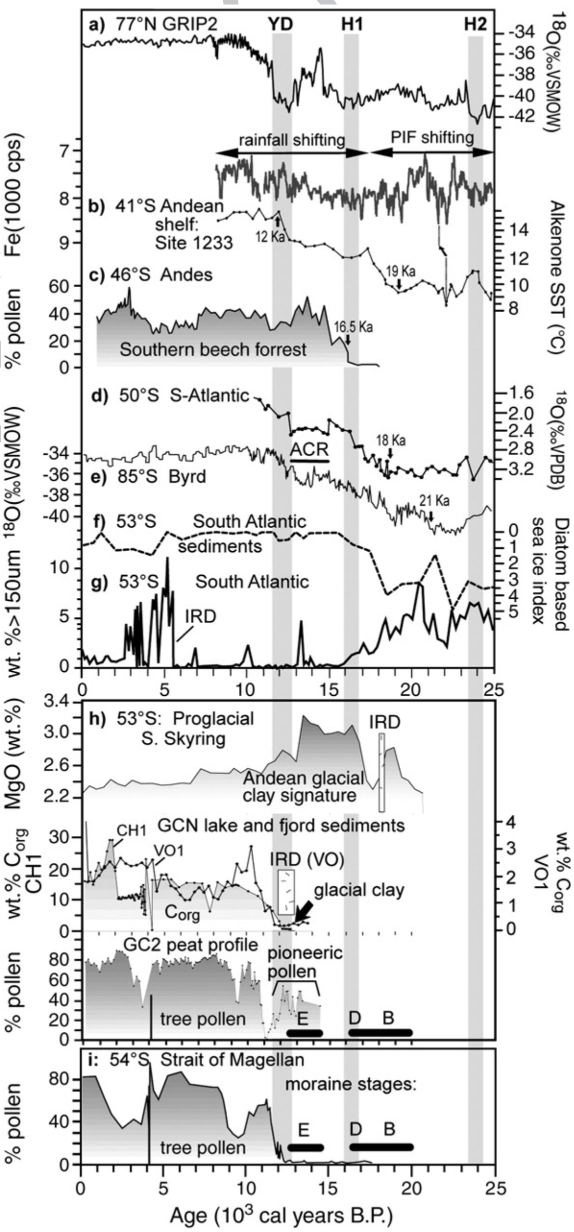

Fig. 8. a–i Comparison of palaeoclimatic data for the last 25,000 yr from the Northern Hemisphere (a: $\delta^{18}O$ from GRIP2, 77°N: Grootes et al., 1993), the Chilean shelf at 41°S (b: Fe content and Alkenone SST's in sediments from ODP Site 1233: Lamy et al., 2004), Southern Andes at 46°S (c: beech forest pollen: Lumley and Switsur, 1993; Bennett et al., 2000), South Atlantic at 50°S (d: $\delta^{18}O$ of *Globigerina buloides* from sediment core RC11–83, primarily reflecting sea surface temperatures: Ninnemann et al., 1999), Antarctica at 85°S (e: $\delta^{18}O$ record from Byrd ice core: Blunier and Brook, 2001), South Atlantic at 53°S (f: diatom-based sea ice reconstruction from core TN 057–13; Stuut et al, in press and g: Lithic grains in sediment core TN 057–13: Hodell et al., 2001) with results from the Gran Campo Nevado area in the Southern Andes at 53°S (h: Andean clay signature with details in Fig. 6a; C_{org} contents in sediment cores VO-1 and CH-1 with details in Figs. 6b and c; tree pollen of peat core GC2 with details in Fig. 6d and in Section 2) and the Strait of Magellan region at 54°S (i: Tree pollen from a peat core: McCulloch et al. 2000). Gray bars indicate the Younger Dryas (YD: Goslar et al., 2000) and Heinrich Events (H1 and H2: e.g. Labeyrie et al., 2003).

Please cite this article as: Kilian, R. et al. Palaeoecological constraints on late Glacial and Holocene ice retreat in the Southern Andes (53°S). Global and Planetary Change (2006), doi:10.1016/j.gloplacha.2006.11.034

and yield Neoglacial moraine building stages in the period of 1220–1460 AD, and subsequently in the 1620s AD and between 1870 and 1910 AD at the GCN (Fig. 5). Neoglacial glacier advances reported above from locations further to the north seem to be missing at GCN. This difference can be explained by a more northward position of the mean course of the Westerlies during the last 4000 yr (Lamy et al., 1998), which could have let to drier conditions at GCN. The LIA moraine system of Glaciar Lengua (Koch and Kilian, in press) shows a similar morphological pattern than sub-aquatic moraine systems from outlet glaciers of GCN and enables to transmit age constraints from moraine systems of Glaciar Lengua to other sub-aquatic moraine complexes around GCN (Fig. 5).

4.2. Differences in glacier retreat between Strait of Magellan and Seno Skyring

While Skyring Glacier lost >84% of length from moraine limit B to limit E (Figs. 2 and 3) in the period from around 17,500 to 14,000 cal. yr B.P. (details in Section 4.1), only 55% of the Magellan glacier length was lost during the same period (Fig. 1). These regional differences can be explained by the morphological characteristics of their respective drainage systems rather than by regional differences in Late Glacial climate change. The Cordillera Darwin drainage area of the Strait of Magellan glacier comprises a much greater accumulation area and is located at higher elevations (up to 2460 m above sea level). In contrast, GCN and other mountains in the Skyring drainage system are of limited extent and at lower elevations. The AAR ratios calculated for the Skyring glacier during LGM moraine limit B (Figs. 1, 3, 7; Section 3.1) suggest that extensive areas of the LGM valley glaciers in the Skyring fjord system protruded above the ELA (200–300 m) and were part of the accumulation area (>50% of the total accumulation area; Fig. 7). But a very low slope of the Skyring Glacier ice surface in the Euston Channel region (Fig. 3, lower profile) made these areas very sensitive to only a slight rise of ELA and would have brought these areas below the ELA. This resulted in a dramatic decrease of accumulation area in the Skyring Glacier system and triggered a much faster recession due to a negative mass balance compared to the Strait of Magellan Glacier system.

4.3. Comparisons of the ice retreat on a global scale

Palaeoclimatic records of the last 25,000 yr from different localities worldwide are compiled in Fig. 8 and compared to results of Gran Campo Nevado area. δ^{18}O pattern from the Greenlandic ice core GRIP2 (Fig. 8a; Grootes et al., 1993) indicate the northern hemispheric cold events of Younger Dryas (YD) and Heinrich Events (H1 and H2). Their possible influences have been discussed controversially for the southernmost Andes (e.g. Lowell et al., 1995; Denton et al., 1999a; Bennett et al., 2000; Moreno et al., 2001). Hajdas et al. (2003) identified a cold event in a lake sediment record from the Andes at 40°S that overlaps the Younger Dryas period, but also preceded YD by 550 cal. yr. In contrast, Alkenone Sea Surface Temperatures (SST's in Fig. 8c) in sediments from Ocean Drilling Program (ODP) Site 1233 from the Chilean continental margin (Lamy et al., 2004) do not show the YD or Heinrich events (Fig. 8c). In the latter record the onset of ocean warming is at around 19,000 cal yr B.P., nearly coeval (18–19 ka) to warming in the South Atlantic, which is indicated by δ^{18}O pattern of *Globigerina buloides* from a sediment core at 50°S (Fig. 8d; Ninnemann et al., 1999).

Based on a comparison with a glacial clay derived high Fe signatures of the ODP Site 1233 sediment record (Fig. 8c), Lamy et al. (2004) have suggested a 1000 yr delayed response of the Patagonian Ice sheet to warming of the Southeast Pacific. In a pollen record from a formerly glaciated area of the Patagonian Ice Field (Fig. 8c; and Lumley and Switsur, 1993; Bennett et al., 2000) a rapid increase of beech forest pollen at around 16,500 cal. yr B.P., suggests also that forest expansion was delayed around 2500 yr relative to the Southeast Pacific warming.

Only a small IRD layer was deposited in the proglacial Seno Skyring between 18,300 to 17,500 cal. yr B.P. (Figs. 6a and 8h), suggesting a rapid recession of Skyring Glacier towards the Euston Channel and moraine system D (Fig. 2). This relatively early glacier recession implies a fast response to Southeast Pacific sea surface warming, probably due to the more limited extent of the Skyring Glacier lobe compared to the Patagonian Ice Field. The beginning of the glacier retreat in the Seno Skyring and Strait of Magellan at around 18,000 to 17,000 cal. yr B.P. (Details in Section 4.1 and Clapperton et al. 1995) occurred around 3000 yr later than the onset of a warming trend in the Antarctic Byrd and Vostok ice cores at 21,000 cal. yr B.P. (Fig. 8e; e.g. Jouzel, 1997; Blunier and Brook, 2001).

The Antarctic Cold Reversal (ACR, ~15,200 to 13,000 cal. yr B.P.; e.g. Steig et al., 1998) is documented in the δ^{18}O pattern of the Byrd ice core from Antarctica at 85°S (Fig. 8e; Blunier and Brook, 2001), in a diatom-based sea ice reconstruction from the South Atlantic at 53°S (Fig. 8f; core TN 057–13; Stuut et al., in press) and by a peak of lithic grains in a sediment record of the

South Atlantic (Fig. 8g; Core TN 057–13; Hodell et al., 2001). The formation of moraine system E between around 15,000 cal. yr B.P. in the Strait of Magellan (Clapperton et al. 1995) and at around 14,000 cal. yr B. P. in the Seno Skyring (Details in Section 4.1) seems to be nearly coeval with the ACR (Figs. 1, 2, 4). At the beginning of the ACR the fast glacier retreat slowed down or stopped in both areas of GCN to Seno Skyring and Strait of Magellan. During the ACR and the YD these glacier systems remained in significantly advanced positions of limit E (Fig. 8h–i; Section 4.1) compared to the Holocene. Further to the North at 40°S in the Chilean Lake District glacier retreat was much more advanced at that time (Moreno et al., 2001; Denton et al., 1999b). This relatively advanced Late Glacial glacier positions in the southernmost Andes could have also been the result of Late Glacial southward migration of the westerly zone and, successively, higher precipitation (Lamy et al. 1998).

Rapid forest expansion (tree pollen in GC2 core of Fig. 8h and Strait of Magellan core of Fig. 8i) and soil formation (strong increase of C_{org} in sediments in CH-1 and VO-1 cores of Fig 8h) first occurs between 12,000 and 11,000 cal. yr B.P. and marks the onset of the Holocene. The climate optimum started at 10,111± 120 cal yr B.P. and lasted until at least 4000 cal. yr. B.P. (Fig. 6d). At least during that time glaciers of Gran Campo Nevado remained behind the limits of LIA. As discussed in Section 4.1, we have also no indications that the mid-Holocene Neoglacial cooling of the South Atlantic (Hodell et al., 2001; Fig. 8g) led glaciers advance to more extensive positions than during LIA. Further to the north (40–52°S) several Neoglacial advances have been documented between 5400 and 1500 cal. yr B.P.. These differences in glacier extent during the Neoglacial may be best explained by variations in snow accumulation, due to a slightly northward shifting of the westerlies after 4000 cal. yr B. P. (Lamy et al., 1998, 1999). This would have resulted in higher accumulation rates along the SPI and the NPI and lower ones at GCN.

5. Conclusions

At Gran Campo Nevado deglaciation after LGM started somewhat earlier than at the Patagonian Ice Field, nearly coeval with the onset of SST warming in the southeast Pacific at around 18,000 cal. yr B.P. (Fig. 8b). Between around 17,500 to <15,000 cal. yr B.P the Seno Skyring Glacier retreated rapidly, losing >80% of its length. This was partly a reaction to the ongoing southern hemispheric warming trend (Fig. 8b, d, e) and caused also a rise of the ELA at Skyring glacier lobe up to a critical altitude, where large proportions (30–50%) of the former accumulation area of the relatively flat glacier surface became ablation area. This loss in accumulation area may have enhanced glacier recession dramatically. During this retreat phase deglaciation may have been also triggered by calving activity in >600 m deep proglacial fjord sections. Around 1000 yr after the onset of the Antarctic Cold Reversal, at around 14,000 cal. yr B.P. (Fig. 8e), the fast Seno Skyring Glacier recession was stopped or at least considerably slowed down. At that time most glaciers of GCN became grounded in deeply incised fjords, which made them less sensitive to climate changes. However, strong SST warming in the southeast Pacific was culminating at around 12,000 cal yr B.P. (Fig. 8b; Lamy et al., 2004), coeval with further Antarctic (Fig. 8e) and South Atlantic warming (Fig. 8d). This may have triggered further retreat of glaciers at Gran Campo Nevado between around 12,000 to 11,000 cal yr B.P., starting probably before the end of YD (Fig. 8h). The Holocene climate optimum between around 10,000 and 5000 cal. yr B.P. (Fig 8h, lower) seems to have been a global phenomenon. Neoglacial conditions, reported from some Glaciers in the Andes (40–50°S), New Zealand and the South Atlantic between 5000 and <1000 cal. yr B.P., were not observed at GCN, probably due to northward shifting of the westerlies (Lamy et al., 1998) and drier condition at the southern tip of South America. In contrast, the LIA has also strongly affected glaciers at GCN as in most other regions of the world.

Acknowledgements

This study was funded by grant numbers Ki-456/6–1/2, Ki-456/8–1 and Schn 680/1–1 of the German Research Society (Deutsche Forschungsgemeinschaft: DFG). Comments from Georg Kaser, Hanns Kerschner and an anonymous reviewer improved the manuscript essentially.

References

Aniya, M., 1995. Holocene glacial chronology in Patagonia: Tyndall and Upsala Glacier. Arctic and Alpine Research 27, 311–322.

Aniya, M., 1996. Holocene variations of Ameghino Glacier, southern Patagonia. The Holocene 6, 247–252.

Aniya, M., Sato, H., Naruse, R., Skvarca, P., Casassa, G., 1996. The use of satellite and airborne imagery to inventory outlet glaciers of the Southern Patagonian Icefield, South America. Photogrammetric Engineering and Remote Sensing 62, 1361–1369.

Bard, E., Rostek, F., Sonzogni, C., 1997. Interhemispheric synchrony of the last deglaciation inferred from alkenone palaeothermometry. Nature 385, 707–710.

Bennett, K.D., Haberle, S.G., Lumley, S.H., 2000. The last Glacial Holocene transition in Southern Chile. Science 290, 325–328.

Blunier, T., Brook, E.J., 2001. Timing of Millennial-Scale Climate Change in Antarctica and Greenland during the Last Glacial Period. Science 291, 109–112.

Blunier, T., Chappelaz, J., Schwander, J., Dällenbach, A., Stauffer, B., Stocker, T.F., Raynaud, D., Jouzel, J., Clausen, H.B., Hammer, C.U., Johnson, S.J., 1998. Asynchrony of Antarctic and Greenland climate change during the last glacial period. Nature 394, 739–743.

Caldenius, C.C., 1932. Las glaciaciones cuaternarios en Patagonia y Tierra del Fuego. Geografiska Annaler 14, 1–164.

Casassa, G., Brecher, H., Rivera, A., Aniya, M., 1997. A century-long record of glacier O'Higgins, Patagonia. Annals of Glaciology 24, 106–110.

Clapperton, C.M., Sudgen, D.E., Kaufmann, D., McCulloch, R.D., 1995. The Late Glaciation in central Magellanstrait, southernmost Chile. Quaternary Research 44, 133–148.

Denton, G.H., Heusser, C.J., Lowell, T.V., Moreno, P.I., Anderson, B.G., Heusser, L.E., Schlüchter, C., Marchant, D.R., 1999a. Interhemispheric linkage of paleoclimate during the Last Glaciation. Geografiska Annaler 81A, 107–153.

Denton, G.H., Heusser, C.J., Lowell, T.V., Schluchter, C., Andersen, B.G., Heusser, L.E., Moreno, P.I., Marchant, D.R., 1999b. Geomorphology, stratigraphy, and radiocarbon chronology of Llanquihue drift in the area of the southern Lake District, Seno Reloncavi, and Isla Grande de Chiloé, Chile. Geografiska Annaler 81A, 167–229.

Faegri, K., Iversen, J., 1989. Textbook of Pollen Analysis. John Wiley & Sons, Chichester.

Fesq-Martin, M., Friedmann, A., Peters, M., Behrmann, J., Kilian, R., in press. Late Glacial and Holocene Vegetation History of the Magellanic rain forest in southwestern Patagonia. Vegetation History and Archeobotany, Accepted in June 2004.

Fischbach, T., Behrmann, J., Kilian, R., 2001. Kinematic constraints for Miocene and younger strike–slip dominated tectonics in the southernmost Andes. Abstracts of the Margins meeting, 02–06.10.2001, Kiel. Schriftenreihe der Deutschen Geologischen Gesellschaft, vol. 14, p. 59.

Franzen, C., Kilian, R., Biester, H., 2004. Natural mercury enrichment in a minerogenic fen evaluation of sources and processes. Journal of Environmental Monitoring 6, 466–472.

Gilli, A., Anselmetti, F.S., Ariztegui, D., Bradbury, P., Kelts, K.R., Markgraf, V., McKenzie, J., 2001. Tracking abrupt climate change in the southern Hemisphere: a seismic stratigraphic study of Lago Cardiel, Argentina (49°S). Terra Nova 13 (6), 443–448.

Godoi, M., Shiraiwa, S., Kohshima, S., Kubota, K., 2002. Firn-core drilling operation at Tyndall glacier, Southern Patagonian Icefield. In: Casassa, G., Speúlveda, F., Sinclair, R. (Eds.), The Patagonian Ice Fields: a unique laboratory for environmental and climate studies. Kluwer Academic Publ., USA, pp. 149–156.

Goslar, T., Arnold, M., Tisnerat-Laborde, N., Czernik, J., Wieckowski, K., 2000. Variations of Younger Dryas atmospheric radiocarbon explicable without ocean circulation changes. Nature 403, 877–880.

Grootes, P.M., Stuiver, M., White, J.W.C., Johnson, S., Jouzel, J., 1993. Comparison of oxygen isotope records from the GISP2 and GRIP Greenland ice cores. Nature 366, 552–554.

Hajdas, I., Bonani, G., Moreno, P., Ariztegui, D., 2003. Precise radiocarbon dating of a Younger Dryas-age cooling in the mid-latitude South America. A step towards climate linkage. Quaternary Research 59, 70–78.

Heusser, C.J., 1989. The westerlies during the Late Glacial Maximum. Quaternary Research 31, 423–425.

Heusser, C.J., Heusser, L., Lowell, T.V., Moreira, M.A., Moreira, S.M., 2000. Deglacial palaeoclimate at Puerto del Hambre, subantarctica, Patagonia, Chile. Journal of Quaternary Research 15, 101–114.

Hodell, D.A., Konfoush, S.L., Shemesh, A., Crosta, X., Charles, C.D., Guildeson, T.P., 2001. Abrupt cooling of Antarctic surface waters and sea ice expansion in the South Atlantic sector of Southern Ocean at 5000 cal. years. B.P. Quaternary Research 56, 191–198.

Hollin, J.T., Schilling, D.H., 1981. Mountain glaciers and small ice caps. In: Denton, G.H., Hughes, T.J. (Eds.), The last great ice sheets. John Wiley & Sons, New York, pp. 179–206.

Hulton, N., Sudgen, A., Payne, A., Clapperton, C.M., 1994. Glacier modelling and the climate of Patagonia during the last glacial maximum. Quaternary Research 42, 1–19.

Jouzel, J., 1997. Validity of the temperature reconstruction from water isotopes in ice cores. Journal of Geophysical Research 102, 26,471–26,487.

Kilian, R., Hohner, H., Biester, H., Wallrabe-Adams, C., Stern, C., 2003. Holocene peat and lake sediment tephra record from the southernmost Andes (53–55°S). Revista Geologica de Chile 30, 47–64.

Koch, J., Kilian, R., in press. Little Ice Age glacier fluctuations, Gran Campo Nevado, southernmost Chile. The Holocene 15 (1). Accepted January 12, 2004.

Labeyrie, L., Cole, J., Alverson, K., Stocker, T., 2003. The history of climate dynamics in the Late Quaternary. In: Alverson, K.D., Bradley, R.S., Pedersen, T.F. (Eds.), Palaeoclimate, Global Change and the Future. Springer, New York, pp. 33–61.

Lamy, F., Hebbeln, D., Wefer, G., Marchant, M., 1998. Reconstructing latitudinal shifts on the southern westerlies from moraine sediment studies along the Chilean continental margin. Pages Newsletters, vol. 2002–2, pp. 8–9.

Lamy, F., Hebbeln, D., Wefer, G., 1999. High-resolution marine record of climate change in mid-latitude Chile during the last 28,000 years based on terrigeneous sediment parameters. Quaternary Research 51, 83–93.

Lamy, F., Kaiser, J., Ninnemann, U., Hebbeln, D., Arz, H.W., Stoner, J., 2004. Antarctic Timing of Surface Water Changes off Chile and Patagonian Ice Sheet Response. Science 304, 1959–1962.

Lliboutry, L., 1998. Glaciares of the wet Andes. In: Williams, R.S., Ferrigno (Eds.), Glaciers of South America, U.S. Geological Survey Professional Paper, U.S.G.S., Washington, pp. 1206–11448.

Lodolo, E., Geletti, R., Sterzai, P., Menichetti, M., Tassone, A., Lippai, H., Hormaechea, J.-L., 2002. Anatomy of a continental transform fault in Tierra del Fuego. EOS 83 (1) January 2002.

Lowell, T.V., Heusser, C.J., Anderson, B.G., Moreno, P.I., Hauser, A., Heusser, L.E., Schlüchter, C., Marchant, D.R., Denton, G.H., 1995. Interhemispheric correlation of Late Pleistocene Glacial Events. Science 269, 1541–1549.

Lumley, S.H., Switsur, R., 1993. Late Quaternary chronology of the Taitao peninsula, southern Chile. Journal of Quaternary Science 8, 161–165.

Markgraf, V., Bradbury, J.P., Schwalb, A., Burns, S.J., Stern, C., Ariztegui, D., Gilli, A., Anselmetti, F.S., Stine, S., Maidana, A., 2003. Holocene palaeoclimates of southern Patagonia: limnological history of Lago Cardiel, Argentina. The Holocene 13, 581–591.

McCulloch, R.D., Davies, S.J., 2001. Late-glacial and Holocene palaeoenvironmental change in the central Strait of Magellan, southern Patagonia. Palaeogeography, Palaeoclimatology, Palaeoecology 173, 143–173.

McCulloch, R.D., Bentley, M.J., Purves, R.S., Hulton, N.R.J., Sudgen, D.E., Clapperton, C.M., 2000. Climatic interferences from glacial and palaeoecological evidence at the last glacial termination, southern South America. Journal Quaternary Science 15, 409–417.

Mercer, J.H., 1970. Variations of some Patagonian glaciers since the Late-Glacial. American Journal of Science 269, 1–25.

Mercer, J.H., 1976. Glacial history of southernmost South America. Quaternary Research 6, 125–166.

Mercer, J.H., 1982. Holocene glacier variations in Southern South America. Holocene Glaciers 18, 35–40.

Moreno, P., Jacobson Jr., G.L., Lowell, T.V., Denton, G.H., 2001. Interhemispheric climate links revealed by a late-glacial cooling episode in southern Chile. Nature 409, 804–808.

Ninnemann, U.S., Charles, C.D., Hodell, D.A., 1999. Origin of global millennial-scale climate events: constraints from the southern ocean deep-sea sedimentary record. In: Mechanisms of Global Climate Change at Millennial Time Scales. Geophyscial Monograph 112, 99–112 Washington, DC (American Geophysical Union).

Porter, S.C., 2000. Onset of neoglaciation in the Southern Hemisphere. Journal of Quaternary Science 15, 395–408.

Rivera, A., Casassa, G., 1999. Volume changes on Pio XI glacier, Patagonia: 1075–1995. Global and Planetary Change 22, 233–244.

Rivera, A., Aravena, J., Casassa, G., 1997. Recent fluctuation of Glaciar Pio XI, Patagonia: discussion of a glacial surge hypothesis. Mountain Research and Development 17, 309–322.

Schneider, C., Glaser, M., Kilian, R., Santana, A., Butorovic, N., Casassa, G., 2003. Weather observations across the Southern Andes at 53°S. Physical Geography 24, 97–119.

Schneider, C., Schnirch, M., Acuña, C., Casassa, G., Kilian, R., this issue-a. Glacier inventory of the Gran Campo Nevado Ice Cap in the Southern Andes and glacier changes observed during recent decades. Global and Planetary Change.

Schneider, C., Kilian, R., Glaser, M., this issue-b. Energy- and mass balance in the ablation area during the summer season at the Gran Campo Nevado Ice Cap. Global and Planetary Change.

Steig, E.J., Brook, E.J., White, J.W.C., Sucher, C.M., Bender, M.L., Lehman, S.J., Morse, D.L., Waddington, E.D., Clow, G.D., 1998. Synchronous climate changes in Antarctica and the North Atlantic. Science 282, 92–95.

Stern, C.R., 1990. Tephrochronology of southernmost Patagonia. National Geographical Research 6, 110–126.

Stern, C.R., Kilian, R., 1996. Role of the subducted slab, mantle wedge and continental crust in the generation of adakites from the Andean Austral Volcanic Zone. Contributions to Mineralogy and Petrology 123, 263–281.

Stuiver, M., Reimer, P.J., 1993. Extended ^{14}C data base and revised CALIB 3.0 ^{14}C Age calibration program. Radiocarbon 35 (1), 215–230.

Stuut, J.-B. W., Crosta, X., vanderBorg K., Schneider, R.R., in press. On the relationship between Antarctic sea ice and southwest African climate during the Late Quaternary. Geology (accepted).

Wardenaar, E.C.P., 1987. A new hand tool for cutting peat profiles. Canadian Journal of Botany 65, 1772–1773.

Warren, C., Aniya, M., 1999. The calving glaciers of the southern South America. Global and Planetary Change 22, 59–77.

Wunderlich, J., Wendt, G., 2001. Advantages of parametric acoustics for the detection of the dredging level in areas with siltation, vol. 7. Workshop on Dredging and Surveying, Scheveningen (The Haag), pp. 1–8. June 7th–8th 2001.

Please cite this article as: Kilian, R. et al. Palaeoecological constraints on late Glacial and Holocene ice retreat in the Southern Andes (53°S). Global and Planetary Change (2006), doi:10.1016/j.gloplacha.2006.11.034